J Mater Sci: Mater Electron (2013) 24:3073–3080
DOI 10.1007/s10854-013-1213-3

Superparamagnetic iron oxide nanoparticles: effect of iron oleate precursors obtained with a simple way

Fatmahan Ozel · Hakan Kockar · Seda Beyaz · Oznur Karaagac · Taner Tanrisever

Received: 24 January 2013 / Accepted: 26 March 2013 / Published online: 25 April 2013

Abstract The objective of the study was to investigate the effect of different amounts of iron oleate precursor with different oleic acid amounts on the properties of the synthesised nanoparticles by thermal decomposition. The iron oleate precursors which formed from oleic acids in the order of 0.5, 1.0, 1.5 and 2.0 g, and 0.1 g iron powder was prepared under 200 °C seperately, using a facile solvothermal method under study. Thermal analysis of iron oleat precursors by a thermogravimetric analysis (TGA) revealed that the different amount of oleic acid was seen to have an impact on the thermal properties of iron oleat complexes. During the synthesis of nanoparticles, iron oleate complex in 1-hexadecane kept refluxing for 3 h under air atmosphere resulting in the formation of nanoparticles. The fourier transform infrared spectra measurements and the TGA analysis disclosed that nanoparticles were coated with oleic acid. To the X-ray diffraction patterns, all samples are iron oxide nanocrystals and their crystal sizes increased from 6.4 to 9.8 nm with decreasing oleic acid. Also, the sizes of nanoparticles were found to be in same range as confirmed with the surface observation by a transmission electron microscope. The magnetic properties obtained from a vibrating sample magnetometer revealed that all nanoparticles are superparamagnetic at room temperature. Also, their saturation magnetizations were up to 33.2 emu/g. It is seen that the nanoparticles are superparamagnetic with the desired structural and corresponding magnetic properties and therefore, they could be thought to be convenient for biomedical applications as the particles can be transferred to aqueous phase.

F. Ozel (✉) · H. Kockar · O. Karaagac
Physics Department, Science and Literature Faculty, Balikesir University, Cagis Yerleskesi, 10145 Balikesir, Turkey
e-mail: fatmahanzel@hotmail.com

H. Kockar
e-mail: hkockar@balikesir.edu.tr

O. Karaagac
e-mail: karaagac@balikesir.edu.tr

S. Beyaz · T. Tanrisever
Chemistry Department, Science and Literature Faculty, Balikesir University, Cagis Yerleskesi, 10145 Balikesir, Turkey
e-mail: sedacan@balikesir.edu.tr

T. Tanrisever
e-mail: taner@balikesir.edu.tr

1 Introduction

Since the novel physical and chemical properties of nanosized particles differ from the bulk materials, they become suitable for broad range of disciplines, including magnetic fluids, data storage, catalysis and bioapplications [1–4]. When the size of nanoparticles is below a critical value, the thermal energy, k_BT exceed the magnetic anisotropic energy barrier and consequently nanoparticles become superparamagnetic [2, 5]. Nanoparticles can also be modified with some coating agents, therefore their sizes can be kept with desired values and become soluble in different solvents and avoid agglomeration which makes them preferable for specific applications such as drug delivery, molecular detection, contrast agents in magnetic resonance imaging [6, 7].

Magnetic nanoparticles can be mostly synthesized with several methods such as thermal decomposition [8], co-precipitation [9], microemulsion [10] and hydrothermal synthesis [11]. Among them, the thermal decomposition is one of the most used method and can be addressed to control of size, shape and monodispersity during synthesis of the nanoparticles [2, 12]. Therefore, the method is useful

to prepare high quality oxide, metal and ferrite nanoparticles compared to other techniques [2]. With the technique, the nanoparticles have been synthesized using decomposition of organometallic precursors i.e. metal oleate ($M(oleate)_x$), metal acetylacetonates ($M(acac)_n$), metal cupferronates (M^xCup_x), or carbonyls in the presence of surfactant with a high boiling point organic solvent [2, 13].

Iron oleate precursor can be synthesized in several ways according to the published procedures [13–15]. NaOH solution in methanol was dropped into the solution which including $FeCl_3.6H_2O$ (or $FeCl_2.4H_2O$) and oleic acid in methanol under magnetic stirring conditions. And, the precipitate of iron oleate was washed with methanol 4–5 times [14]. In another study, the solution of $FeCl_3.6H_2O$ and sodium oleate in a mixture of solvents composed of ethanol, hexane, distilled water was heated to reflux for 4 h under stirring, and also, the iron oleate phase was washed several times to eliminate by-products including NaCl [13]. Bronstein et al. investigated a solution containing the same chemicals [13] was heated to 70 °C and stirred at this temperature for 4 h under an argon flow [15]. The current way for synthesizing precursor was simply obtained from a mixture of different amounts of oleic acid and the iron powder (0.1 g) in hexane under 200 °C temperature for 3 h. To the thermal analysis by thermogravimetric analysis, the different amounts of oleic acid were seen to affect the thermal properties of iron oleat precursors. The work done by now has demonstrated more complicated ways of iron oleat precursor synthesis than that of the current investigation which uses a simple way.

The ways of improving electromagnetic devices are the improving the properties of existing materials or developing a new class of magnetic materials by considering the experimental conditions. The nanoparticle properties vary depending on the synthesis conditions such as the reaction time, reaction temperature and type of the surfactant and precursor, and especially the ratio of precursor and surfactant[2, 13], which remains challenging. Thus, it would be significant to carry out a study of iron oleat variation using a thermal decomposition synthesis to enrich and better understand the influence of the different amounts of oleic acid on the chemical, crystal and magnetic characterizations of these nanocrystals.

Therefore, upon the study of the effect of oleic acid variation on iron oleat precursor, the present investigation focuses on the properties of nanoparticles synthesised by thermal decomposition method to understand and control superparamagnetic nature of the nanoparticles at the atomic level through the amount of oleic acid manipulations. The iron oleates, obtained from oleic acid ranging from 0.5 to 2.0 g, were used as precursor. The magnetic iron oxide nanoparticles, in crystal diameter decreasing from 9.8 to 6.4 nm with increasing oleic acid from 0.5 to 2.0 g, were easily synthesized using the current precursors. It is also disclosed that, saturation magnetizations of the nanoparticles obtained from magnetic measurements were found to be compatible with the chemical and physical changes caused by the iron oleat precursors synthesized at different amounts of oleic acids. Thus, it can be said that the nanoparticles with the desired magnetic properties were coated with oleic acid molecules, and hence they could be protected from oxidation and agglomeration.

2 Experimental

Oleic acid (Sigma-Aldrich, 99 %), hexane (Merck, 95 %) and iron powder (Merck) were used for the synthesis of iron oleate. 1-Hexadecane (Aldrich, 92 %) was used for the synthesis of iron oxide nanoparticles. All reagents in this work are in analytical grade.

The iron oleate complexes were prepared only by using iron powder and oleic acid in hexane at high temperature under study. The oleic acid in the range of 0.5, 1.0, 1.5 and 2.0 g were dissolved in 10 ml hexane, separately. And, each solution and 0.1 g iron powder transferred into a Teflon-lined stainless steel autoclave. Then, the autoclave was put into oven and kept at 200 °C for 6 h, and then cooled to room temperature, naturally. This is followed by removing the remaining iron powder from the iron oleat with a magnet. Finally, hexane was evaporated in the air.

The iron oleate precursors were obtained from 0.5, 1.0, 1.5 and 2.0 g oleic acids and were used for the synthesis of iron oxide nanoparticles (labeled as samples N1, N2, N3 and N4), respectively. Also, the last precursor acquired from 2.0 g. oleic acid was washed several times with ethanol and acetone, and then dried in an oven at 40 °C. After extraction, the product was seen to be a waxy solid [15] and used for the production of nanoparticles (N5).

The iron oleat precursors with the order of 0.5, 1.0, 1.5 and 2.0 g oleic acid were added to 10 ml 1-hexadecane, seperately and each solution was heated to the reflux and then kept at that temperature for 3 h. It is observed that the colour of solution turned black. This is followed by cooling the solution to room temperature. Then the nanoparticles were precipitated with 40 ml acetone and 10 ml hexane together to complete the synthesis process of the nanoparticles, and at the end, they were dispersed in chloroform.

The samples were characterized by Fourier transform infrared spectroscopy (FTIR, Perkin Elmer-1600 Series). For iron oleate samples, the solid sample was prepared by pelletizing with KBr powder while for the FTIR study of the nanoparticles, first nanoparticles dispersed in chloroform solutions were dropped on KBr disks, and then the chloroform evaporated in the air, finally dry pellets with

nanoparticles were obtained. And, TGA was performed with diamond series from Perkin Elmer Instruments. The crystal structure of nanoparticles was identified by using X-ray powder diffraction (XRD, PANalytical's X'Pert PRO) with angle ranging from 20° to 80°. Beside, the size and shape of the nanoparticles were obtained from transmission electron microscope (HRTEM, FEI TECNAI G2 F30 model) images. For obtaining TEM images of the nanoparticles, the samples were prepared as dilute chloroform solutions were dropped onto copper grid and dried in air. The magnetic properties of nanoparticles were obtained by vibration sample magnetometer (VSM, ADE EV9 Model) in the field range up to ±20 kOe with 1 Oe increments.

3 Results and discussion

Iron-oleate complexes were obtained using an easy way of production and used as precursor, and a standard procedure by the thermal decomposition technique [12, 15] was conducted to synthesize the nanoparticles. Since individual iron oleate complex consisted of free oleic acid, no extra stabilizer was used during the synthesis of the nanoparticles. All results are presented in Table 1.

3.1 Characterizations of iron oleate precursor

The effect of the oleic acid on the properties of iron oleat precorsor was studied using the FTIR and TGA. The structures of all iron oleate samples were identified with the FTIR spectroscopy. First two FTIR spectrums of the iron oleates synthesized with low (0.5 g) and (b) high (2.0 g) oleic acid were presented in Fig. 1a, b, respectively. And, the spectrum of the washed iron oleate obtained from 2.0 g oleic acid was presented in Fig. 1c. For comparison, the FTIR spectrum of pure oleic acid sample was added as Fig. 1d. As observed in pure oleic acid spectrum in Fig. 1d, the carboxylic acid dimers displayed a broad and intense O–H stretching absorption in the region of 3,300–2,500 cm^{-1} [16]. The iron oleates synthesized with 0.5 and 2.0 g oleic acid in Fig. 1a, b displayed narrower and less intense O–H stretching absorption in the same region than that of the FTIR spectrum of pure oleic acid in Fig. 1d. However, for the washed iron oleate obtained from 2.0 g oleic acid in Fig. 1c, the O–H stretching absorption disappeared but a new band at 3,468 cm^{-1} was observed, probably due to the washing process [15]. Two sharp bands at 2,924 and 2,854 cm^{-1}, which were superimposed on the O–H stretching band, were attributed to the asymmetric CH_2 and the symmetric CH_2 stretches, respectively [17]. All samples had υ(=C–H) stretching band at 3,004 cm^{-1} as in [18] irrespective of the amount of oleic acid. For iron oleat samples, the carboxylate ion gives rise to two bands: around 1,650–1,510 cm^{-1} for the asymmetrical stretching band and at about 1,400 cm^{-1} for the symmetrical stretching band [16]. Due to the extraction of the iron oleate, the bands of 1,596 and 1,522 cm^{-1} overlapped and hence became less evident in Fig. 1c. The interaction between the carboxylate and metal atom is categorized as four types: ionic, monodentate, bidentate(chelating), or bridging [18]. The coordination type can be interpreted from the wavenumber separation, Δ, between the antisymmetric, $\upsilon_{as}(COO^-)$, and the symmetric, $\upsilon_s(COO^-)$, stretching bands. For $\Delta > 200$ cm^{-1} a monodentate ligand is expected, and for $\Delta < 110$ cm^{-1} a bidentate. For a bridging ligand, Δ is between 140 and 200 cm^{-1} [18]. Comparing the spectrums of the iron oleate with 0.5 and 2.0 g, and the pure oleic acid sample, two new peaks were appeared around 1,522 and 1,596 cm^{-1} which corresponds to the antisymmetric, $\upsilon_{as}(COO^-)$ bands. However, the band at 1,445 cm^{-1} was the symmetric, $\upsilon_s(COO^-)$, stretching. As Δ = 1,596–1,445 cm^{-1}=151 cm^{-1} and Δ = 1,522–1,445 cm^{-1} = 77 cm^{-1}, these were indicating that oleic acid was attached bridging and bidentate fashion, respectively. The C=O group absorbs in the region of 1,711 cm^{-1} and this band points to presence of free oleic acid [15]. Accordingly, Fig. 1a, b showed that the iron oleates with 0.5 and 2.0 g contained free oleic acid. However, 1,711 cm^{-1} peak nearly disappeared for the washed sample, see Fig. 1c. This indicated that a large part of free oleic acid removed after the washing process.

Table 1 Preparation conditions of iron oleate and properties of iron oxide nanoparticles

Nanoparticle samples	Oleic acid (g)	Nanoparticle sizes		Magnetic parameters	
		d_{XRD} (nm)	d_{TEM} (nm ± Δnm)	M_s (emu/g)	H_s (Oe)
N1	0.5	9.8	10.2 ± 3.2	6.0	1,918
N2	1.0	9.5	–	17.2	2,608
N3	1.5	6.9	–	19.4	4,835
N4	2.0	6.4	7.6 ± 2.9	22.5	6,606
N5[a]	2.0	7.7	8.2 ± 2.2	33.2	4,538

[a] After the iron oleate precursor was washed several times with ethanol and acetone and dried in an oven at 40 °C

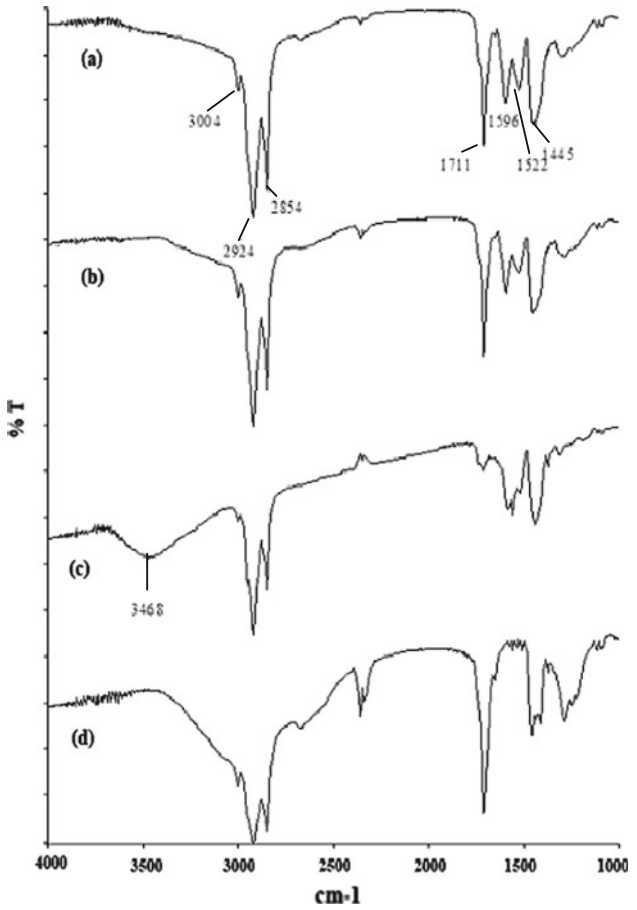

Fig. 1 FTIR spectra of iron oleates prepared with **a** 0.5 g, **b** 2.0 g oleic acid, **c** the washed iron oleate obtained from 2.0 g oleic acid and **d** pure oleic acid

The thermal properties of the synthesized iron oleate complexes were obtained with TGA. The TGA spectrums of the iron oleat samples presented the similar types of peaks with slightly different percentage mass losses which are near to each other. The TGA spectrum of iron oleate complexes synthesized with 1.5 and 2.0 g oleic acid and the washed iron oleate synthesized from 2.0 g oleic acid were presented in Fig. 2a–c, respectively. To confirm the existence of free oleic acid in the iron oleate complex, the TGA of pure oleic acid was also measured and shown in Fig. 2d. In the figure, the decomposition temperature of pure oleic acid was found to be between 200 and 300 °C. But, there were two derivative peaks in the TGA curves of samples in Fig. 2a, b. In Fig. 2a, first peak was at 260 °C with the percentage mass loss of 52 %, which correspond to decomposition of free oleic acid and refers to the weakly bounded oleic acid [19]. These findings were also supported by the FTIR analysis. With the percentage mass loss (37 %), the second peak at 357 °C probably indicates the decomposition of iron oleate precursor. In Fig. 2b, the first peak with the percentage mass loss of 58.7 % was at 294 °C while for the second peak with the percentage mass loss of 34.5 % was at 353 °C. For sample in Fig. 2b, free oleic acid moved the peak a little forward since the sample contained more free oleic acid than that of sample in Fig. 2a. According to the weight losses for sample shown in Fig. 2c, the first mass loss occurred at 210 °C is probably due to the removal of the surface adsorbed ethanol, acetone and free oleic acid, and therefore the loss was around 10 %. With the percentage mass losses (32 and 41 %), the second and third peaks, indicating the decomposition of iron oleate complex, were at about 361 and 556 °C and, respectively.

3.2 Effect of iron oleat precursors on the synthesis of iron oxide nanoparticles

The influence of oleic acid on the properties of iron oxide nanoparticles was studied using the structural (FTIR, TGA, XRD and TEM) and also magnetic (VSM) measurement techniques. The FTIR spectrums for all samples were obtained. The spectrum of samples N1 and N4 (obtained with low (0.5 g) and (b) high (2.0 g) oleic acid) and sample N5 (obtained from the washed iron oleate from 2 g oleic acid) were given in Fig. 3a–c, respectively, see also Table 1. The main difference between these samples was that the peak intensity of the patterns of sample N1 and N4 were higher than that of sample N5. First two sharp bands at 2,923 and 2,852 cm^{-1} were ascribed to the asymmetric CH_2 stretch and the symmetric CH_2 stretch, respectively, as indicated in [17]. Beside, no band observed at 1,711 cm^{-1} indicated that there were no free oleic acid, and oleic acid molecules covalently bounded to the nanoparticles surface as shown in Fig. 1a–c. In the spectrums, the peaks in the range from 1,600 and 1,400 cm^{-1} are ascribed to the carboxylate group of oleate ion coordinated to Fe ion [19]. In the samples, the Δ (1,637–1,465 cm^{-1}=172 cm^{-1}) was attributed to the bridging effect between these two peaks. Final broad band observed at 595 cm^{-1} corresponds to the vibration of the Fe–O functional group [13]. The spectrums confirmed that the surface of all magnetic nanoparticles was capped by oleic acid.

Figure 4 showed of the TGA curves of oleic acid coated nanoparticles (sample N5). Two derivative peaks were observed in the TGA curve. The first peak with the percentage mass loss (6 %) was at 244 °C due to the decomposition of weakly bounded oleic acid. The weight loss (20 %) measured for the second peak between 310 and 550 °C represented the loss of the covalently bonded oleic acid molecules. Due to the removal of the surface coating oleic acid and adsorbed ethanol, acetone and free oleic acid, the total loss of the sample was ≥20 %.

The XRD patterns of the nanoparticles (samples N1–N5) were measured. The samples N1, N4 and N5 were

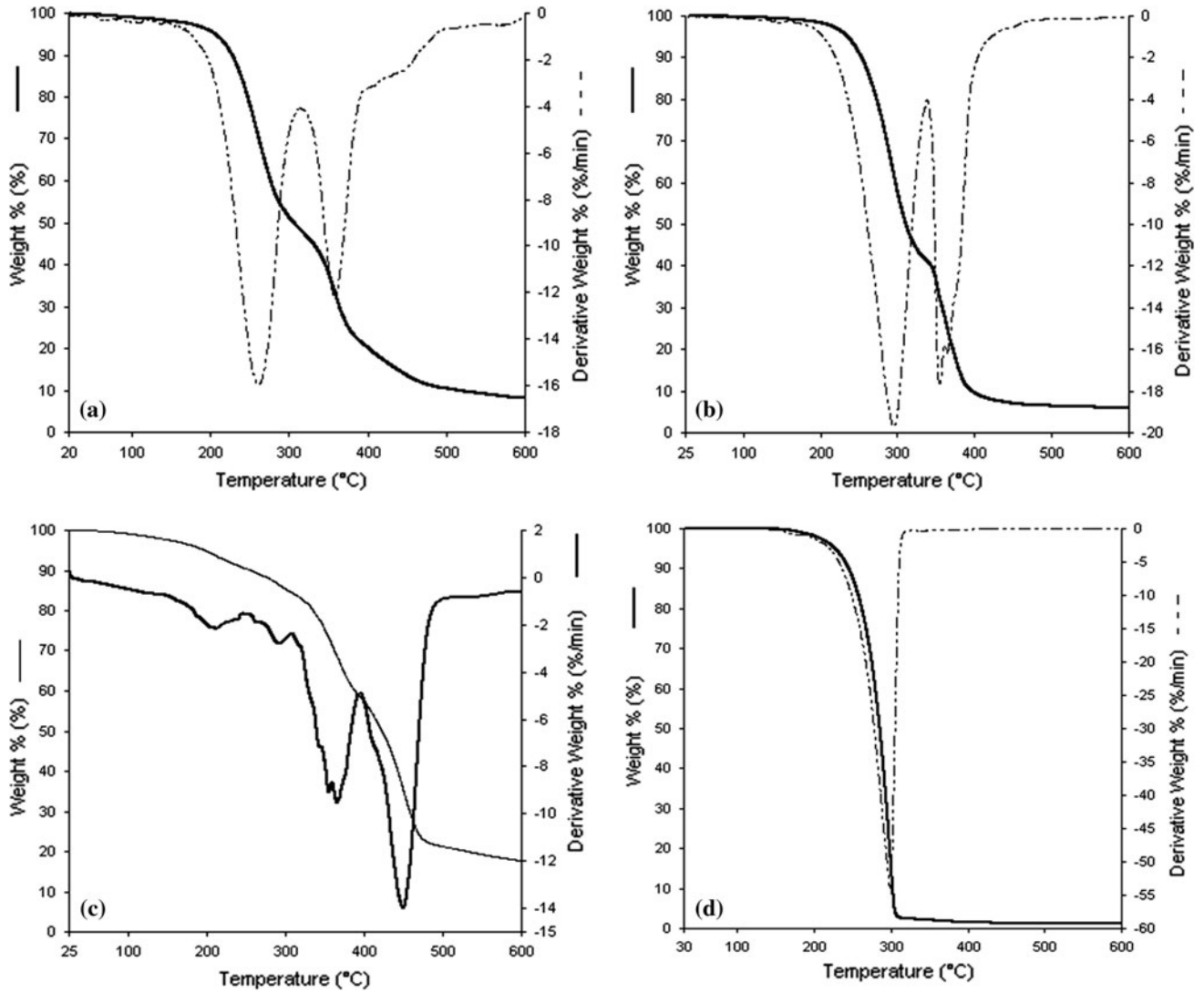

Fig. 2 TGA/DTA curves of iron oleates prepared with **a** 1.5 g, **b** 2.0 g oleic acid, **c** the washed iron oleate obtained from 2.0 g oleic acid and **d** pure oleic acid

presented in Fig. 5a–c. In the XRD patterns of the nanocrystals, the (220), (311), (400), (422), (511), (440) reflections at around $2\theta \approx 30°$, 35°, 43°, 53°, 57° and 63° were assigned to the spinel structure of the magnetite, Fe_3O_4 (JCPDS no. 19-0629) or maghemite, γ-Fe_2O_3 (JCPDS no. 39-1346) since their XRD patterns are nearly identical [9]. The rest of the samples (N2 and N3) were also seen to have the same patterns. The average crystallite sizes, d_{XRD}, calculated by Scherrer's equation [20] from the most intense (311) peak of the XRD patterns, decreased from 9.8 nm to 6.4 nm as the amount of oleic acid increased.

The TEM images in Fig. 6 revealed that iron oxide nanoparticles were independently dispersed and they have the narrow size distribution. The mean sizes, d_{TEM}, obtained from the TEM images for samples N1, N4 and N5 were 10.2 ± 3.2 nm, 7.6 ± 2.9 nm and 8.2 ± 2.2 nm, respectively. The sizes are found to be consistent with the XRD values. The shapes of the nanoparticles were spherical. Besides, the iron oxide nanoparticles in Fig. 4c have less spherical surface shape than the nanoparties in Fig. 6a, b due to probably the removal of the oleic acid.

Up to now the iron oxide nanoparticles have different properties. As for magnetic properties, room temperature magnetisation measurements were conducted to analyse the properties obtaining the magnetisation parameters as saturation magnetisation, M_s, saturation field, H_s, remanence, M_r and coercivity, H_c from magnetisation curves. In Fig. 7, the magnetization curves of all the samples are shown at $\pm$10kOe. It is seen that the M_r and H_c obtained from the curves are zero and hence all samples were identified as superparamagnetic. The M_s (6.0–22.5 emu/g)

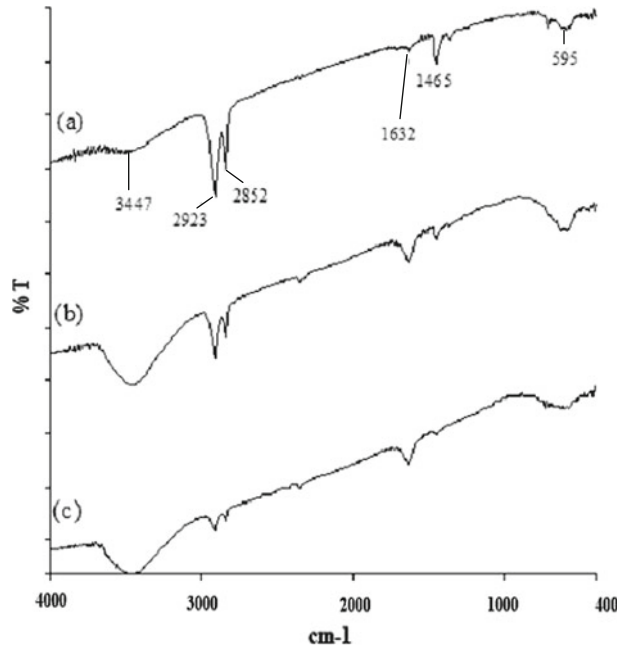

Fig. 3 FTIR spectra of nanoparticles, samples **a** N1, **b** N4 and **c** N5

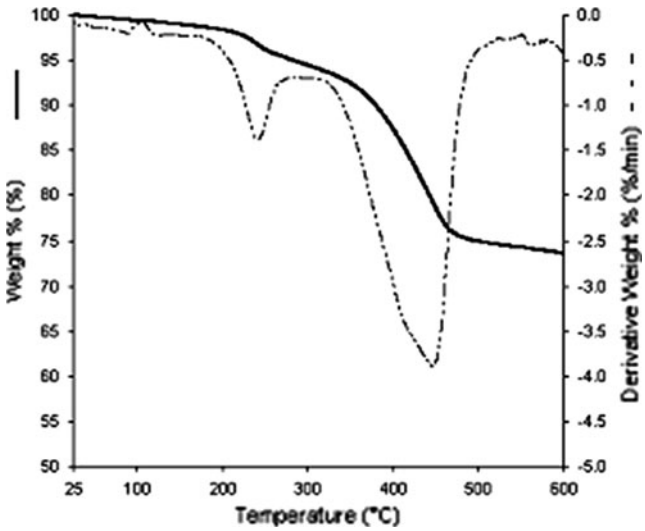

Fig. 4 TGA/DTA curves of nanoparticles of sample N5

and H_s (1,918–6,606 Oe) increased as the oleic acid increased from 0.5 to 2.0 g. These indicate that the easy axis of magnetisation is the direction of decreasing H_s due to the decrease of oleic acid. Therefore, it is harder to magnetise the samples at high oleic acid than the low one. The M_s of all samples were found to be lower than that of the bulk maghemite (73.5 emu/g) and magnetite (92 emu/g) which were most likely due to the existence of organic coating agents and smaller size of particles [21, 22]. Also, in our study, more effective explanation for obtaining low M_s may have come from the oleic acid coating agents on

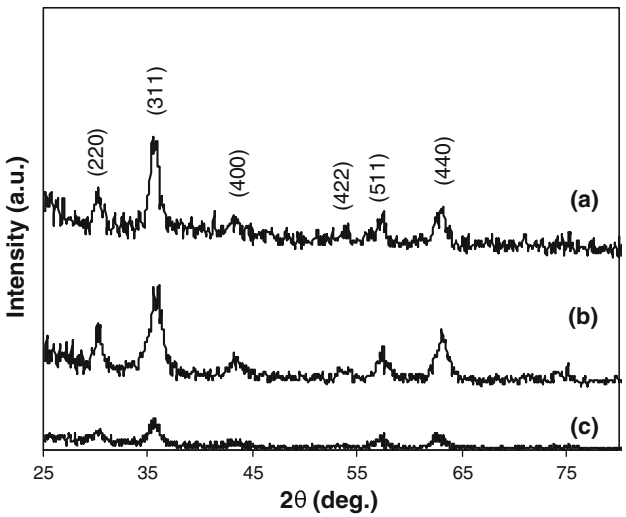

Fig. 5 The XRD pattern of iron oxide nanoparticles for samples **a** N1, **b** N4 and **c** N5

surface of the nanoparticles since the magnetic moment obtained from the VSM is divided by the whole sample mass to calculate the M_s values. Thus, the washed nanopartiles from oleic acid (sample N5), exhibited relatively high $M_s = 33.2$ emu/g. This result indicates that capping agents, which have negative effect against saturation magnetization, have removed during the washing process. The absolute M_s of the samples could be calculated using the TGA findings. As an example, the M_s for iron oxide core of N5 was calculated as 45 emu/g since the weight percentage for iron oxide core was 74 % according to the TGA results. It is disclosed that the increase of H_s is a result of a decrease in the crystalline sizes caused by oleic acid amount.

4 Conclusions

The study investigated the effect of the newly developed precursors on the properties of the nanoparticles synthesised by thermal decomposition. The iron oleate precursor was formed from oleic acid and iron powder under high temperature. To the structure of iron oleat complexes by the FTIR, the $\Delta = 151$ cm^{-1} and $\Delta = 77$ cm^{-1}, indicate that oleic acid was attached bridging and bidentate fashion, respectively. The chemical and thermal analysis of the precursors by the FTIR and the TGA, respectively have disclosed that the different amount of oleic acid have an impact on the properties of iron oleat precursors. As for the nanoparticles, the physical and magnetic caharcterisations were studied with respect to amount of oleic acid. Also, the nanoparticles were chemically characterized by the FTIR and the TGA. The FTIR measurements indicated that surface of the nanoparticles were capped with oleic acid,

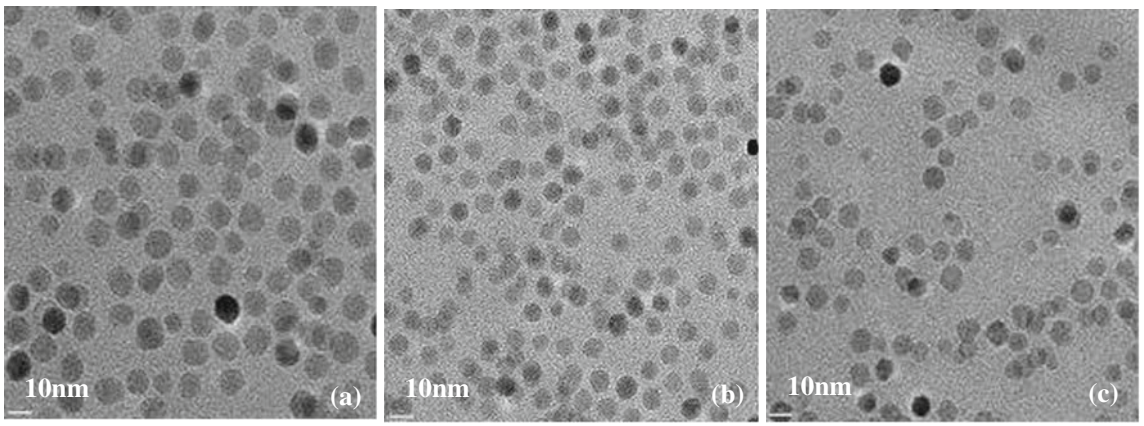

Fig. 6 TEM images of iron oxide nanoparticles, samples **a** N1, **b** N4, **c** N5

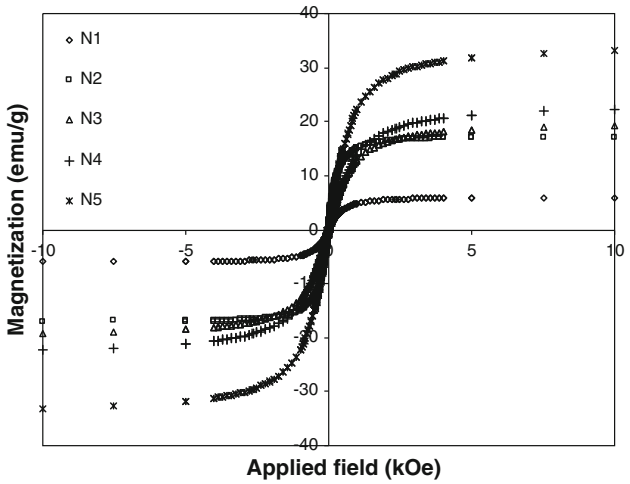

Fig. 7 The magnetization curves of all samples of nanoparticles at room temperature

and the bridging modes were observed. The XRD analysis disclosed that all samples are iron oxide nanocrystals and their crystal sizes were in the order of 6.4–9.8 nm with the decrease of oleic acid. Transmission electron microscope images showed that the nanoparticles were spherical in shape, and the mean size of nanoparticles decreased from 10.2 ± 3.2 nm to 7.6 ± 2.9 nm as the amounts of oleic acid increased. The magnetic properties were also studied in accordance with the changes of structural properties caused by the oleic acid. Synthesised nanoparticles were superparamagnetic at room temperature and their saturation magnetizations increased up to 33.2 emu/g with the increase of oleic acid. The saturation field increased with decreasing crystalline sizes caused by oleic acid.

Acknowledgments This work was supported by Balıkesir University Research Grant no. BAP 2008/04 and TUBITAK 109T017. The authors would like to thank State Planning Organisation, Turkey under Grant no 2005K120170 for VSM system. The authors also thank the Chemistry Department, Balikesir University, Turkey for FTIR, XRD and TGA measurements, and the National Nanotechnology Research Center (UNAM), Bilkent University for TEM analysis.

References

1. Y.-W. Jun, J.-W. Seo, J. Cheon, Nanoscaling laws of magnetic nanoparticles and their applicabilities in biomedical sciences. Acc. Chem. Res. **41**, 179–189 (2008)
2. A.-H. Lu, E.L. Salabas, F. Schüth, Magnetic nanoparticles: synthesis, protection, functionalization and application. Angew. Chem. Int. Ed. **46**, 1222–1244 (2007)
3. T.K. Jain, M.A. Morales, S.K. Sahoo, D.L. Leslie-Pelecky, V. Labhasetwar, Iron oxide nanoparticles for sustained delivery of anticancer agents. Mol. Pharm. **2**, 194–205 (2005)
4. F. Kockar, S. Beyaz, S. Sinan, H. Kockar, D. Demir, S. Eryılmaz, T. Tanrisever, O. Arslan, Paraoxonase 1-bound magnetic nanoparticles: preparation and characterizations. J. Nanosci. Nanotechnol. **10**, 7554–7559 (2010)
5. D.L. Leslie-Pelecky, R.D. Rieke, Magnetic properties of nanostructured materials. Chem. Mater. **8**, 1770–1783 (1996)
6. W. Wu, Q. He, C. Jiang, Magnetic iron oxide nanoparticles: synthesis and surface functionalization strategies. Nanoscale Res. Lett. **3**, 397–415 (2008)
7. M. Colombo, S. Carregal-Romero, M.F. Casula, L. Gutiérrez, M.P. Morales, I.B. Böhm, J.T. Heverhagen, D. Prosperi, W.J. Parak, Biological applications of magnetic nanoparticles. Chem. Soc. Rev. **41**, 4306–4334 (2012)
8. J. Park, E. Lee, N.-M. Hwang, M. Kang, S.C. Kim, Y. Hwang, J.-G. Park, H.-J. Noh, J.-Y. Kim, J.-H. Park, T. Hyeon, One-nanometer-scale size-controlled synthesis of monodisperse magnetic iron oxide nanoparticles. Angew. Chem. Int. Ed. **44**, 2872–2877 (2005)
9. S. Lefebure, E. Dubois, V. Cabuil, S. Neveu, R. Massart, Monodisperse magnetic nanoparticles: preparation and dispersion in water and oils. J. Mater. Res. **13**, 2975–2981 (1998)
10. C.R. Vestal, Z.J. Zhang, Synthesis of $CoCrFeO_4$ nanoparticles using microemulsion methods and size-dependent studies of their magnetic properties. Chem. Matter. **14**, 3817–3822 (2002)
11. S. Ge, X. Shi, K. Sun, C. Li, C. Uher, J.R. Baker Jr., M.M. Banaszak Holl, B.G. Orr, Facile hydrothermal synthesis of iron oxide nanoparticles with tunable magnetic properties. J. Phys. Chem. **113**, 13593–13599 (2009)
12. J. Park, K. An, Y. Hwang, J.-G. Park, H.-J. Noh, J.-Y. Kim, J.-H. Park, N. Hwang, T. Hyeon, Ultra-large-scale syntheses of monodisperse nanocrystals. Nat. Mater. **3**, 891–895 (2004)

13. A.G. Roca, M.P. Morales, C.J. Serna, Synthesis of monodispersed magnetite particles from different organometallic precursors. IEEE Trans. Magn. **42**, 3025–3029 (2006)
14. N.R. Jana, Y. Chen, X. Peng, Size- and shape-controlled magnetic (Cr, Mn, Fe, Co, Ni) Oxide Nanocrystals via a simple and General Approch. Chem. Matter. **16**, 3931–3935 (2004)
15. L.M. Bronstein, X. Huang, J. Retrum, A. Schmucker, M. Pink, B.D. Stein, B. Dragnea, Influence of iron oleate complex structure on iron oxide nanoparticle formation. Chem. Matter **19**, 3624–3632 (2007)
16. R.M. Silverstein, G.C. Bassler, T.C. Morrill, *Spectrometric Identification of Organic Compounds* (Wiley, New York, 2005)
17. N. Wu, L. Fu, M. Su, M. Aslam, K.C. Wong, V.P. Dravid, Interaction of fatty acid monolayers with cobalt nanoparticles. Nano Lett. **4**, 383–386 (2004)
18. F. Söderlind, H. Pedersen, R.M. Petoral Jr., P.-O. Kall, K. Uvdal, Synthesis and characterisation of Gd_2O_3 nanocrystals functionalised by organic acids. J. Colloid Interface Sci. **288**, 140–148 (2005)
19. S.G. Kwon, Y. Piao, J. Park, S. Angappane, Y. Jo, N.-M. Hwang, J.-G. Park, T. Hyeon, Kinetics of monodisperse iron oxide nanocrystal formation by "Heating-Up" process. J. Am. Chem. Soc. **129**, 12571–12584 (2007)
20. Y.C. Han, H.G. Cha, C.W. Kim, Y.H. Kim, Y.S. Kang, Synthesis of highly magnetized iron nanoparticles by a solventless thermal decomposition method. J. Phys. Chem. **111**, 6275–6280 (2007)
21. D.K. Lee, Y.H. Kim, X.-L. Zhang, Y.S. Kang, Preparation of monodisperse Co and Fe nanoparticle using precursor of M^{2+}-$Oleate_2$ (M = Co, Fe). Curr. Appl. Phys. **6**, 786–790 (2006)
22. S.-Y. Zhao, D.K. Lee, C.W. Kim, H.G. Cha, Y.H. Kim, Y.S. Kang, Synthesis of magnetic nanoparticles of Fe_3O_4 and $CoFe_2O_4$ and their surface modification by surfactant adsorption. Bull. Korean Chem. Soc. **27**, 237 (2006)